

Proper Orthogonal Decomposition for Particle-in-Cell Simulations

Julio L. Nicolini, Dong-Yeop Na, and Fernando L. Teixeira
 ElectroScience Laboratory, The Ohio State University
 Columbus, OH 43212 USA
 email: {delimanicolini.1, na.94, teixeira.5}@osu.edu

Abstract—The Proper Orthogonal Decomposition technique for model order reduction is applied to electromagnetic particle-in-cell algorithms. The resulting low-dimensional model can be used to achieve solutions with acceptable accuracy and reduced computational costs in problems with charged particle beams.

I. INTRODUCTION

Particle-in-Cell (PIC) algorithms have been used for a variety of problems involving charged particles and beams (see e.g. [1], [2] and references therein), but they remain an expensive technique in terms of computational resources. The Proper Orthogonal Decomposition (POD) is a technique that lowers the computational cost of numerical experiments by projecting the solution into a (smaller) space spanned by a number of representative modes [3]–[6]. Due to previous success in applying the POD to EM simulations [7], [8], in this work the POD is applied to a finite-element time-domain (FETD) PIC algorithm.

II. PROPER ORTHOGONAL DECOMPOSITION

POD-based models are construed with sampled data-points from the quantity of interest [3], [5], which can be obtained from a numerical or practical experiment. In the present case, electric field and magnetic flux data is obtained from a full FETD-PIC simulation via construction of a “snapshot” matrix encoding spatial and temporal variations of each quantity.

Let \mathbf{u} denote either 1-D array of DoFs, i.e., $\mathbf{u}^n = \mathbf{e}^n$ or $\mathbf{b}^{n-\frac{1}{2}}$. Then a snapshot matrix for \mathbf{u} with l entries is constructed by harvesting the values of all DoFs for the transient solution at specific sampling points n_i , $i \in \{1, 2, \dots, l\}$ and arranging them side-by-side so that $[\mathbf{A}_{\mathbf{u}}]_{i,j} = u_i^{n_j}$. The snapshot matrices can be decomposed via singular value decomposition (SVD), viz. [3]

$$[\mathbf{A}_{\mathbf{u}}] = [\mathbf{U}_{\mathbf{u}}] \cdot [\mathbf{\Sigma}_{\mathbf{u}}] \cdot [\mathbf{V}_{\mathbf{u}}]^T, \quad (1)$$

where $[\mathbf{U}_{\mathbf{u}}]$ and $[\mathbf{V}_{\mathbf{u}}]$ are unitary matrices and $[\mathbf{\Sigma}_{\mathbf{u}}]$ is a rectangular diagonal matrix with main diagonal elements containing the singular values $\sigma_{\mathbf{u},i}$ of $[\mathbf{A}_{\mathbf{u}}]$ in descending order and zero elsewhere. The columns of $[\mathbf{U}_{\mathbf{u}}]$ form a set of orthonormal vectors $\{\psi_{\mathbf{u},1}, \psi_{\mathbf{u},2}, \dots, \psi_{\mathbf{u},N_{\text{DoF},\mathbf{u}}}\}$ that can be regarded as a basis for the spatial dynamics, while the columns of $[\mathbf{V}_{\mathbf{u}}]$ form a set of orthonormal vectors $\{\phi_{\mathbf{u},1}, \phi_{\mathbf{u},2}, \dots, \phi_{\mathbf{u},l}\}$ that can be regarded as a basis for the temporal dynamics [6], [9].

Choosing a reduced number $d_{\mathbf{u}}$ of modes from the set of spatial dynamics creates the reduced set $\{\Psi_{\mathbf{u},i}\}_{i=1}^{d_{\mathbf{u}}}$ or, in matrix form, $[\Psi_{\mathbf{u}}]$, which can be used to lower the dimension of the numerical simulation.

III. ELECTROMAGNETIC MODEL REDUCTION

The time update equations for the discrete degrees of freedom (DoFs) of the fields in the FETD-PIC simulation are given by (details in [1], [10], [11])

$$\mathbf{b}^{n+\frac{1}{2}} = \mathbf{b}^{n-\frac{1}{2}} - \Delta_t [\mathbf{C}] \cdot \mathbf{e}^n, \quad (2a)$$

$$[\star_{\epsilon}] \cdot \mathbf{e}^{n+1} = [\star_{\epsilon}] \cdot \mathbf{e}^n + \Delta_t \left([\mathbf{C}]^T \cdot [\star_{\mu-1}] \cdot \mathbf{b}^{n+\frac{1}{2}} - \mathbf{i}^{n+\frac{1}{2}} \right), \quad (2b)$$

which can be projected onto the POD basis via

$$\mathbf{e}^n \approx [\Psi_{\mathbf{e}}] \cdot \alpha_{\mathbf{e}}^n, \quad \mathbf{b}^{n-\frac{1}{2}} \approx [\Psi_{\mathbf{b}}] \cdot \alpha_{\mathbf{b}}^{n-\frac{1}{2}}, \quad (3)$$

which allows the update equations to take the reduced form

$$\alpha_{\mathbf{b}}^{n+\frac{1}{2}} = \alpha_{\mathbf{b}}^{n-\frac{1}{2}} - \Delta_t [\Psi_{\mathbf{b}}]^T \cdot [\mathbf{C}] \cdot [\Psi_{\mathbf{e}}] \cdot \alpha_{\mathbf{e}}^n, \quad (4a)$$

$$\alpha_{\mathbf{e}}^{n+1} = \alpha_{\mathbf{e}}^n + \Delta_t \left([\Psi_{\mathbf{e}}]^T \cdot [\star_{\epsilon}] \cdot [\Psi_{\mathbf{e}}] \right)^{-1} \cdot \left([\Psi_{\mathbf{e}}]^T \cdot [\mathbf{C}]^T \cdot [\star_{\mu-1}] \cdot [\Psi_{\mathbf{b}}] \cdot \alpha_{\mathbf{b}}^{n+\frac{1}{2}} - [\Psi_{\mathbf{e}}]^T \cdot \mathbf{i}^{n+\frac{1}{2}} \right), \quad (4b)$$

where not only the DoFs themselves are reduced, but the system matrix inversion $([\Psi_{\mathbf{e}}]^T \cdot [\star_{\epsilon}] \cdot [\Psi_{\mathbf{e}}])^{-1}$ is also reduced due to its much smaller size, allowing for explicit update in the scheme via direct inversion without need of approximations.

IV. NUMERICAL EXAMPLE

Consider a vacuum-filled square cavity with perfect magnetic conductor (PMC) boundary conditions. The cavity walls each measure 1 [m], and it has initial zero field conditions and no particles. The cavity is discretized with an irregular triangular mesh containing $N_0 = 1633$ nodes, $N_1 = 4768$ edges and $N_2 = 3136$ faces. Electrons are injected into the cavity at the lower boundary with velocity $v_0 = 1 \times 10^4$ [m/s] and absorbed at the upper boundary, with an external bias set to $V_b = 1.5 \times 10^4$ [V]. Each computational particle represents 100,000 physical electrons, and five particles are injected every five time-steps according to a uniform random distribution at $y = 0$ between $x = 0.4$ and $x = 0.6$. The time step interval is $\Delta_t = 1 \times 10^{-11}$ and the simulation is run for $n = 100,000$

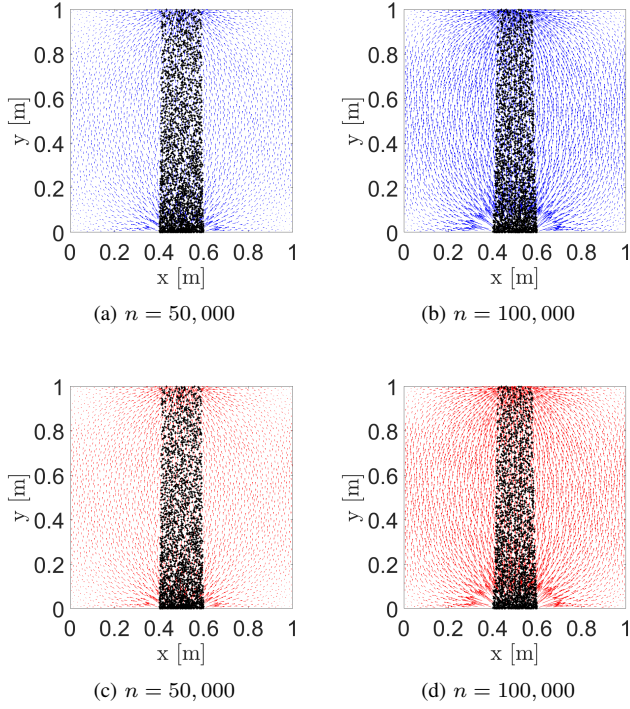


Fig. 1. Comparison between electric field lines and electron positions between the full FETD simulation (top) and the reduced POD simulation (bottom).

time steps. The snapshot matrices are construed by harvesting DoF values every 500 time steps until $n = 20,000$.

Fig. 1 shows a comparison between electric field lines and particle positions in the FETD and POD simulations, while Fig. 2 shows the spectrum of singular values for the electric field and the magnetic flux, as well as the relative global error between the two simulations, calculated via

$$\delta_e^n = \frac{1}{N_s} \left\| \frac{\mathbf{E}_{\text{fetd}}^n - \mathbf{E}_{\text{pod}}^n}{\left(\frac{1}{N_t} \sum_n \mathbf{E}_{\text{fetd}}^n \right)} \right\|_2, \quad (5)$$

where subscripts fetd and pod stand for quantities of the full and reduced-order simulations, respectively, N_t is the total number of time-steps in the simulation and N_s is the total number of spatial samples used in the error measurement. Good accuracy (relative error lower than 0.1%) is accomplished by the reduced simulation at lower computational cost (6 modal DoFs as opposed to $N_1 + N_2 = 7,904$ in the full simulation for both fields).

ACKNOWLEDGEMENT

This work was supported in part by NSF grant ECCS-1305838, DTRA grant HDTRA1-18-1-0050, and OSC grants PAS-0061 and PAS-0110.

REFERENCES

[1] D.-Y. Na, H. Moon, Y. A. Omelchenko, and F. L. Teixeira, "Local, explicit, and charge-conserving electromagnetic particle-in-cell algorithm on unstructured grids," *IEEE Trans. Plasma Sci.*, vol. 44, pp. 1353–1362, 2016.

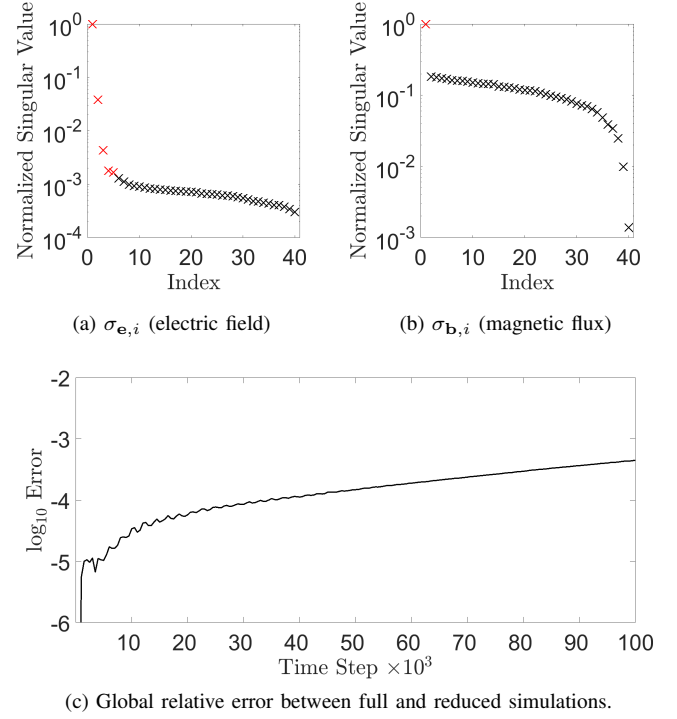


Fig. 2. Details on the singular values for (a) electric field and (b) magnetic flux, as well as (c) global error between simulations. The reduced model used 5 modes for the electric field and 1 mode for the magnetic flux; the singular values associated with the retained modes are marked in red.

[2] D.-Y. Na, H. Moon, Y. Omelchenko, and F. Teixeira, "Relativistic extension of a charge-conservative finite element solver for time-dependent maxwell-vlasov equations," *Physics of Plasmas*, vol. 25, no. 1, p. 013109, 2018.

[3] Y. Liang, H. Lee, S. Lim, W. Lin, K. Lee, and C. Wu, "Proper orthogonal decomposition and its applications part i: Theory," *Journal of Sound and vibration*, vol. 252, no. 3, pp. 527–544, 2002.

[4] A. Chatterjee, "An introduction to the proper orthogonal decomposition," *Current science*, pp. 808–817, 2000.

[5] M. Rathinam and L. R. Petzold, "A new look at proper orthogonal decomposition," *SIAM Journal on Numerical Analysis*, vol. 41, no. 5, pp. 1893–1925, 2003.

[6] N. Aubry, "On the hidden beauty of the proper orthogonal decomposition," *Theoretical and Computational Fluid Dynamics*, vol. 2, no. 5-6, pp. 339–352, 1991.

[7] Z. Luo and J. Gao, "A pod reduced-order finite difference time-domain extrapolating scheme for the 2d maxwell equations in a lossy medium," *Journal of Mathematical Analysis and Applications*, vol. 444, no. 1, pp. 433–451, 2016.

[8] K. Li, T.-Z. Huang, L. Li, S. Lanteri, L. Xu, and B. Li, "A reduced-order discontinuous galerkin method based on pod for electromagnetic simulation," *IEEE Transactions on Antennas and Propagation*, vol. 66, no. 1, pp. 242–254, 2018.

[9] N. Aubry, R. Guyonnet, and R. Lima, "Spatiotemporal analysis of complex signals: theory and applications," *Journal of Statistical Physics*, vol. 64, no. 3-4, pp. 683–739, 1991.

[10] H. Moon, F. L. Teixeira, and Y. A. Omelchenko, "Exact charge-conserving scatter-gather algorithm for particle-in-cell simulations on unstructured grids: A geometric perspective," *Comput. Phys. Commun.*, vol. 194, pp. 43–53, 2015.

[11] J. Kim and F. L. Teixeira, "Parallel and explicit finite-element time-domain method for Maxwell's equations," *IEEE Trans. Antennas Propag.*, vol. 59, pp. 2350–2356, 2011.